

LIBRARY
RESEARCH REPORTS DIVISION
NAVAL POSTGRADUATE SCHOOL
MONTEREY, CALIFORNIA 93940

CAD
Cout

RAY DIRECTIONS, WAVE NORMALS
AND RIGOROUS RAY TRACING

Edward R. Floyd

Oceanography Department*
Naval Postgraduate School
Monterey, California 93940

1983

ABSTRACT

Herein some sample exact effective sound velocity profiles for rigorous ray tracing are developed numerically. The equations of motion for rigorous ray tracing are developed and it is shown that in general a ray is not normal to the wave surfaces of constant phase.

* Visiting scientist in the Environmental Acoustics Research Group.
Permanent Address: Naval Ocean Systems Center, San Diego,
California 92152.

RAY DIRECTIONS, WAVE NORMALS
AND RIGOROUS RAY TRACING

Edward R. Floyd

Oceanography Department*
Naval Postgraduate School
Monterey, California 93940

ABSTRACT

Herein some sample exact effective sound velocity profiles for rigorous ray tracing are developed numerically. The equations of motion for rigorous ray tracing are developed and it is shown that in general a ray is not normal to the wave surfaces of constant phase.

*Visiting scientist in the Environmental Acoustics Research Group.
Permanent Address: Naval Ocean Systems Center, San Diego,
California 92152.

INTRODUCTION

A rigorous ray tracing theory has already been developed to first order where it was shown that an effective sound velocity profile was in general dependent upon frequency.¹ A higher order theory for wave mechanics has also been developed in one dimension.² Exact albeit numerical wave functions have recently been developed for bound states (i.e., trapped modes in underwater acoustics) in one dimension where the turning point (vertex depth in underwater acoustics) of the phase integral have been shown to recede to ∞ for indices of refraction that remain finite and where the effective action variable (the phase integral around the branch cut between the turning points for the N^{th} eigenvalue, $N = 1, 2, 3, \dots$) in units of phase has been shown to be N cycles for the N^{th} trapped mode.³ The modes have been shown to be numerically exact within the limits of computer round-off.^{3,4}

In this exposition, the terminology "rigorous ray tracing" denotes an exact, albeit numerical ray tracing while "classical ray tracing" denotes the conventional ray tracing that is valid in the short wavelength or infinite frequency limit.

Herein we apply some of these developments in wave mechanics to underwater acoustics in order to generate for depth-dependent sound velocity profiles a rigorous ray theory that is exact, albeit numerical, and that is mutually consistent with a normal mode theory. The objectives of this investigation are to gain insight into the physics of rigorous ray tracing from a few examples of the exact effective sound velocity profile, to develop the correct equations of motion for the ray, and to show that the ray directions in general are not orthonormal to the wave surfaces of constant phase (i.e.,

the wave normals and the ray directions for the same points are not in general parallel).

In this exposition we assume that the sound velocity profile is a function of depth only and that for finite depths, the inverse square of the sound velocity profile is finite. The surface is at zero depth. The earth is assumed to be flat and we assume a bottomless ocean. Herein cylindrical coordinates are used and we assume the source is located on the z -axis at some depth, z_s . Hence we have azimuthal symmetry. We also assume that the sound source is a point harmonic source whose frequency is ω in radians per second. All numerical computations were based upon a Runge-Kutta fourth-order technique with a step size of 25 m.

In Section I of this exposition, we develop Hamilton's principal function, S , for rigorous ray tracing which is based upon the alternative development presented in Appendix A of Ref. 1. (Heretofore S had been cited as the effective Hamilton's principal function.) Subsequently we develop the equations of motion by the Hamilton-Jacobi process and we develop the relationship between the ray direction and wave normal. In Section II we generate some sample exact effective sound velocity profiles, $C_e(z)$ from a simple sound velocity profile, $C(z)$. From these exact samples, we glean some insight into the behavior and application of rigorous ray tracing. A brief outline of applicable portions of classical ray tracing is presented in Appendix A.

I. THEORY

Here we shall develop the equations of motions for a ray and show that the ray is in general not normal to the acoustical wave surfaces of constant phase. Here for convenience and without loss of generality, we express the sound velocity profile, C , which has been assumed to be a function of depth only, by the form

$$C(z) = [A - B(z)]^{-1/2}$$

where z is depth and where A , a real constant, and $B(z)$, a real function, are chosen such that at the source depth, z_s , of the sound, $C(z_s) = A^{-1/2}$.

As $C(z)$ is only depth dependent, the Helmholtz equation is separable such that the z component may be expressed

$$\partial^2 \theta(z) / \partial z^2 + \omega^2 [A - C_m^{-2} - B(z)] \theta(z) = 0 \quad (1)$$

where θ is a scalar, ω is frequency in radians per second, C_m^{-2} is the real separation constant such that $A > C_m^{-2}$. In addition, C_m is also the vertex (WKB turning point) velocity. Let us use an ansatz, which has been inspired by the WKB approximation, for θ of the form

$$\theta_{\pm} = (A - C_m^{-2} - \beta)^{-1/4} \exp[\pm i \int^z \omega(A - C_m^{-2} - \beta)^{1/2} dz']. \quad (2)$$

Substituting Eq. (2) into Eq. (1) generates a nonlinear differential equation for our new variable, β , expressed by

$$\beta + \frac{1}{4\omega^2} \frac{\partial^2 \beta / \partial z^2}{(A - C_m^{-2} - \beta)} + \frac{5}{16\omega^2} \left(\frac{\partial \beta / \partial z}{A - C_m^{-2} - \beta} \right)^2 = B(z). \quad (3)$$

The initial conditions for β require that Huygen's construction may be accomplished in the neighborhood near the source.¹ Therefore the initial conditions are

$$\beta|_{z=z_s} = B(z_s) = 0$$

and

$$\frac{\partial \beta}{\partial z}|_{z=z_s} = \frac{dB}{dz}|_{z=z_s}.$$

From the form of Eq. (3), we see that β is a function of z , ω and C_m . We note that for trapped modes Eq. (3) has a nodal-type critical point³ such that $\beta \rightarrow A - C_m^{-2}$ from below as $z \rightarrow \infty$. This node at $z = \infty$ moves the vertex depth (turning point) for the ray (for flat earth) for rigorous ray tracing from the WKB vertex depth to infinity. Further investigation of β is deferred to Section II.

The phase of our ansatz is given by

$$\begin{aligned} & \int^z \omega [A - \beta(z', \omega, C_m) - C_m^{-2}]^{1/2} dz' \\ &= \int^z \omega [C_e^{-2}(z', \omega, C_m) - C_m^{-2}]^{1/2} dz' = \omega W(z, \omega, C_m) \end{aligned} \quad (4)$$

where by analogy to Eq. (A4) W is Hamilton's characteristic function for rigorous ray tracing and C_e is defined to be the effective velocity given by

$$C_e(z, \omega, C_m) = [A - \beta(z, \omega, C_m)]^{-1/2}. \quad (5)$$

We develop Hamilton's principal function, S , for rigorous ray tracing as

$$S = W(z, \omega, C_m) + \frac{r}{C_m} \quad (6)$$

because range is a cyclic coordinate and azimuth is symmetric. By Eqs. (4) and (6) and by using $\partial S / \partial r = (1/C_m)$ to change C_e temporarily from a function of C_m to $\partial S / \partial r$, we have the Hamilton-Jacobi equation for rigorous ray tracing expressed by

$$\partial S / \partial r - [C_e^{-2}(z, \omega, \partial S / \partial r) - (\partial S / \partial z)^2]^{1/2} = 0. \quad (7)$$

There is a subtle difference between Eqs. (7) and (A2) because the range dependence, which only appears explicitly in Eq. (A2), appears in Eq. (7) both explicitly and in C_e implicitly. Thus, even though C_m^{-2} is a separation constant for the Helmholtz equation, C_m is no longer a separation constant for Eq. (7) (albeit Eq. (6) is still valid for cyclic r), but $(1/C_m)$ still is a transformed momentum of the Hamilton-Jacobi process for both Eqs. (7) and (A3). Hence C_e is in general anisotropic.

Either S or W (at the worker's option) may act as the generating function from which the equations of motion for rigorous ray tracing may be derived. But we note that the ansatz may be expressed as

$$\theta_{\pm} = (\partial W / \partial z)^{-1/2} \exp \pm i \omega W.$$

As the ansatz describes the normal mode (the analogous exact, albeit numerical, quantum mechanical eigenfunctions have been so described elsewhere^{3,4}), we may derive the eigenfunctions from W by quantizing the product of ω and

the action variable for rigorous ray tracing to be N cycles of phase, $N = 1, 2, 3, \dots$. Hence W is the keystone by which we may derive mutually consistent normal mode and rigorous ray tracing theories thus rendering a unifying principle.

The wave normals for rigorous ray tracing are given by the gradients of S which for cylindrical symmetry renders

$$\nabla S = [C_e^{-2}(z, \omega, C_m) - C_m^{-2}]^{1/2} \hat{i}_z + C_m^{-1} \hat{i}_r.$$

Thus the wave normal is embedded in a radial-vertical plane and the wave normal may be described by the deflection/elevation (D/E) angle, ψ . This D/E angle is given by

$$\psi = \tan^{-1} \left[\left(\frac{C_m}{C_e} \right)^2 - 1 \right]^{1/2} = \cos^{-1} \left(\frac{C_e}{C_m} \right) \quad (8)$$

which may be expressed in a manner similar to Snell's law for classical ray tracing as

$$C_m = \frac{C_e(z, \omega, C_m)}{\cos \psi(z)} \quad (8')$$

where C_m is an implicit function as opposed to the classical ray tracing, Eq. (A1), where it is an explicit function.

We now derive the continuous motion for rigorous ray tracing for the ray passing depth z . By the Hamilton-Jacobi process the range r that a ray passes depth z is given for cylindrical symmetry by

$$\frac{\partial S}{\partial (1/C_m)} = 0 = \frac{\partial W}{\partial (1/C_m)} + r$$

or

$$r = \int_{z_s}^z \frac{c_e [1 - (c_m/c_e)^3 (\partial c_e/\partial c_m)]}{(c_m^2 - c_e^2)^{1/2}} dz, \quad (9)$$

where the Hamilton-Jacobi constant coordinate, which normalizes range with respect to source location, is zero for sources located on the z -axis. It is noted that the integral in Eq. (9) is a line integral and that one must integrate along the branch cut and around any encountered branch points (i.e., vertex depths) onto the next Riemann sheet. The node in Eq. (3) at $z = \infty$ for trapped rays induces $c_e \rightarrow c_m$ from below and $\partial c_e/\partial c_m \rightarrow 1$ from below as $z \rightarrow \infty$. Thus the vertex depth for the ray is at infinite depth. Nevertheless, the range quadrature, Eq. (9), for rigorous ray tracing remains bound and integrable for trapped rays as shown in Section II. Furthermore in the limit $c_e \rightarrow c_m$ by L'Hospital's rule, the integrand in Eq. (9) goes to zero.

For cylindrical symmetry by Eq. (9), the ray also is embedded in a radial-vertical plane. The D/E angle, ϕ , for the ray for rigorous ray tracing by Eq. (9) is given by

$$\begin{aligned} \phi &= \cot^{-1} \left(\frac{dr}{dz} \right) \\ &= \cot^{-1} \left\{ \frac{c_e [1 - (c_m/c_e)^3 (\partial c_e/\partial c_m)]}{[c_m^2 - c_e^2]^{1/2}} \right\} \end{aligned} \quad (10)$$

which in general differs from ψ as given by Eq. (8). Hence the ray direction is not parallel to the wave normal. There is a precedent for rays not being normal to the wave surfaces of constant phase or W in the optics of

anisotropic crystals. In a preceding paragraph of this section, it has been shown that in general C_e is anisotropic.

At the source, $\partial C_e / \partial C_m = 0$ in order to satisfy the boundary conditions for Eq. (3). Hence at the source, we have by Eqs. (8) and (10) that $\psi(z_s) = \phi(z_s)$.

Equation (10) is Snell's law for the ray for rigorous ray tracing. Because Eq. (3) has a node at $z = \infty$, we have that $\psi \rightarrow 0$ and $\phi \rightarrow 90^\circ$ as $z \rightarrow \infty$. Hence the ray is parallel to the wave surface at the vertex point at $z = \infty$ for rigorous ray tracing.

It is noted that Ref. 1 needs correction because Eq. (8) of this exposition was given in Ref. 1 as the applicable modification of Snell's law without distinguishing between wave normals and ray directions. Nevertheless all applications in Ref. 1 of Snell's law, which were based upon an effective sound velocity profile developed only to first order, are correct because to first order only, C_e is a function of both z and ω but not C_m . Thus a first-order C_e is isotropic. We note that if C_e is independent of C_m , then Eq. (10) reduces to Eq. (8).

We offer a caution with regard to rigorous ray tracing with an effective sound velocity profile as given by $C_e = (A - \beta)^{-1/2}$ where β is the solution to Eq. (3). The worker is admonished to use C_e only in a Hamilton-Jacobi process (regrettably, it does not render correct results when C_e is substituted for C into a Lagrangian or Hamiltonian calculus of variation process).

II. ANALYSES OF SAMPLE APPLICATIONS

Let us assume a sound velocity profile, $C(z)$, such that

$$C(z) = [(1420)^2 - \frac{0.036z}{(1420)^3}]^{-1/2}, \quad z > 0$$

where C is in meters per second and z is in meters. The source depth is assumed to be zero. This profile was chosen for investigation because (1) it represents the profile that is dominated by the pressure gradient in the absence of a thermocline and (2) in a perturbation expansion² the first order calculation of C_e is identical to C . Here we examine C_e for various values of C_m and ω . Subsequently we rigorously trace a particular ray to exhibit its penetration of the classically forbidden region beyond the WKB vertex depth and to exhibit the divergence between the ray direction and wave normal.

Let us now numerically solve Eq. (3) and exhibit by Fig. 1 the effective sound velocity profile, C_e , for a harmonic surface source ($z_s = 0$) with $\omega = 50$ rad/s for rays with initial D/E angles [note $\psi(z_s) = \phi(z_s)$; $z_s = 0$] of 5° , 10° , 15° (i.e., $C_m = 1425.4242$ mps, 1441.9058 mps, 1470.0922 mps respectively). In Fig. 1, the nodal behavior of Eq. (3) is manifested by $C_e \rightarrow C_m$ from below as $z \rightarrow \infty$. Hence we observe that the vertex depth recedes to $z = \infty$. Well above the WKB vertex depths, C_e and C are good approximations of each other (this may not be true for less-well-behaved profiles¹), and by the initial conditions C_e is tangent to C at the source depth z_s . For completeness, the actual sound velocity profile, C , is also exhibited on Fig. 1. Note that in the limit where the initial D/E angle goes to 90° , (i.e., $C_m \rightarrow \infty$), then C_e would mimic C as closely as possible for the value of A (here $A^{1/2} = 1420$ m/s) but still C_e would not go to C .

However in the limit $A \rightarrow \infty$ and the initial D/E angle is not 0° , then $C_e \rightarrow C$ (the analogy in quantum mechanics would be the infinite energy case).

In Fig. 2 we exhibit various effective sound velocity profiles for surface sources with an initial D/E angle of 10° (i.e., $C_m = 1441.9058$ mps) and with $\omega = 5$ rad/s, 50 rad/s, 500 rad/s. The sound velocity profile, C , is also exhibited on Fig. 2. We note that for finite depths above the WKB vertex depth C_e approaches C as ω increases and that for finite depths below the WKB vertex depth, C_e approaches C_m as ω increases. In the limit $\omega \rightarrow \infty$, we have that

$$\lim_{\omega \rightarrow \infty} C_e \rightarrow \begin{cases} C, & C \leq C_m \\ C_m, & C > C_m. \end{cases} \quad (11)$$

Let us now investigate the correspondence principle of how rigorous ray tracing goes to classical ray tracing in the high frequency limit. In the case $\omega \rightarrow \infty$ and below the WKB vertex depth (which is the classical ray tracing vertex depth) in the classical forbidden region, the ray direction is parallel to the wave front and so the ray is embedded in a wave surface of constant phase. Hence below the WKB vertex point for $\omega \rightarrow \infty$, the ray senses a constant phase and thus the ansatz, Eq. (2), in the forbidden region has a constant phase despite $\omega \rightarrow \infty$, that is, the integrand of Eq. (4) behaves such that $(A - C_m^{-2} - \beta) \rightarrow 0$ as $\omega \rightarrow \infty$. The boundary condition for infinite frequency for the solution to Eq. (1) requires that in the classical forbidden region that $\theta(z) = 0$ for z below the WKB vertex depth. Therefore we have that

$$\theta = (\theta_+ - \theta_-)/2, \quad \omega \rightarrow \infty$$

for depths below the WKB vertex depth

which goes to zero⁷ by L'Hospital's rule despite the singularity in the amplitude factor in both θ_+ and θ_- as given by Eq. (2). Thus for $\omega \rightarrow \infty$, there is no penetration below the WKB vertex depth, and by Eq. (11) below the WKB vertex depth the integrand of the range quadrature, Eq. (9), for rigorous ray tracing is zero by L'Hospital's rule while above the WKB vertex point Eq. (9) reduces to the range quadrature, Eq. (A5), for classical ray tracing as $\partial C_e / \partial C_m \rightarrow 0$. Thus in the limit $\omega \rightarrow \infty$, rigorous ray tracing corresponds to classical ray tracing [the quantum mechanical analogy³ is the correspondence principle for $(\hbar^2/2\mu) \rightarrow 0$ where \hbar is Planck's constant and μ is mass].

We exhibit on Fig. 3 the rigorous ray trace for a surface source for $\omega = 50$ rad/s and the $\phi(z_s) = \psi(z_s) = 10^\circ$ (i.e., $C_m = 1441.9058$ mps) by numerically evaluating Eq. (9). The corresponding classical ray trace is exhibited also on Fig. 3 for a half-cycle in range (i.e., until the first WKB vertex depth is encountered at $z = 1189.1117$ m) where classically $r = 13,490.938$ m. While the corresponding rigorous ray trace has its vertex depth at $z = \infty$ which is not exhibited, we report that the range for the corresponding rigorous ray trace to the first vertex depth has been evaluated to be $13,557 \pm 6$ m. This infers that classical ray tracing for one-half cycle for these conditions has an estimated error of 65 m in range or about 0.498% in range.

We note that while the vertex depth for rigorous ray tracing has receded to infinity, the range quadrature has remained finite. We also report that the time quadrature, which is the action variable for a full cycle remains finite as inferred by the analogous quantum mechanical effective action variable remaining finite for bound states of the symmetric bi-linear potential whose eigenfunctions are offset Airy functions.^{3,4}

On Fig. 4 we exhibit as a function of depth the wave normal, ψ , and the ray angle, ϕ , for the ray that was rigorously traced on Fig. 3. For

classical ray tracing, which also is exhibited on Fig. 4, the wave normal and ray angle are equivalent. We note that well above the WKB vertex depth in the classically allowed region both ψ and ϕ approach their classical ray-tracing prediction. But below the WKB vertex depth we have that as $z \rightarrow \infty$, then $\psi \rightarrow 0$ and $\phi \rightarrow 90^\circ$. Hence, as $z \rightarrow \infty$, the ray travels parallel to the wave front as noted earlier.

APPENDIX A
CLASSICAL RAY TRACING

In this appendix, we outline the development of the Hamilton-Jacobi theory of classical ray tracing in the short wavelength, λ , or high frequency limit (i.e., $\lambda \rightarrow 0$ or $\omega \rightarrow \infty$) and show that the ray path is always normal to the wave fronts. Here we assume that the sound velocity profile, C , is only dependent upon depth, z , that the earth is flat and that the ocean is bottomless. We use cylindrical coordinates and assume the source is located on the z -axis at depth z_s .

We start with the Lagrangian, L , for ray tracing that for azimuthal symmetry is given in cylindrical coordinates by

$$L(z, \dot{z}) = \frac{(1 + \dot{z}^2)^{1/2}}{C(z)}$$

where $\dot{z} = dz/dr$ where r is the radial coordinate and for sources on the z -axis r determines range. The conjugate momentum, P_z , with respect to depth is given by

$$P_z = \frac{\partial}{\partial \dot{z}}(L) = \frac{\dot{z}}{C(z)(1 + \dot{z}^2)^{1/2}} = \frac{\sin \phi}{C(z)}$$

where ϕ is the depression-elevation (D/E) angle of the ray (for azimuthal symmetry, the ray is embedded in the radial-vertical plane). As L is not an explicit function of range, r , the classical ray-tracing Hamiltonian, H ,

is given by

$$\begin{aligned} H(z, p_z) &= \dot{z}p_z - L = -[C^2 - p_z^2]^{1/2} \\ &= -\frac{\cos \phi}{C(z)} = -\frac{1}{C_m} \end{aligned} \quad (A1)$$

which gives Snell's law since H is a constant of the motion for H independent of r . The constant of the motion for any particular ray may be expressed in terms of its vertex velocity, C_m . The Hamilton-Jacobi equation for classical ray tracing is given by

$$\frac{\partial S}{\partial r} + H(z, \frac{\partial S}{\partial z}) = 0$$

or

$$\frac{\partial S}{\partial r} - [C(z)^{-2} - (\frac{\partial S}{\partial z})^2]^{1/2} = 0 \quad (A2)$$

where S is Hamilton's principal function for classical ray tracing and has the dimensionality of time. Thus the surface of constant S represents a wave surface. Because the only range dependence is restricted to the $\frac{\partial S}{\partial r}$ term in Eq. (A2), we may assume a solution of the form

$$S(z, C_m, r) = W(z, C_m) + r/C_m \quad (A3)$$

where W is Hamilton's characteristic function for classical ray tracing. From Eqs. (A2) and (A3), W may be expressed as

$$W \doteq \int^z [C^{-2} - C_m^{-2}]^{1/2} dz. \quad (A4)$$

The wave normal is given by the direction of the gradient of Hamilton's principal function, S , which by Eqs. (A1) and (A2) is given for azimuthal symmetry as

$$\nabla S = \frac{1}{C_m} \hat{i}_r + [\frac{1}{C^2} - \frac{1}{C_m^2}]^{1/2} \hat{i}_z.$$

For azimuthal symmetry the wave normal is embedded in a radial-vertical plane and the wave-normal may be described by the D/E angle, ψ , of the wave normal as given by

$$\tan^{-1} \left[\frac{C_m^2}{C^2} - 1 \right]^{-1/2} = \psi$$

But the equation of motion for the ray for classical ray tracing from a source on the z -axis is given for azimuthal symmetry by

$$\frac{\partial S}{\partial (1/C_m)} = 0 = \int_{z_s}^z \frac{-C dz'}{[C_m^2 - C^2]^{1/2}} + r \quad (A5)$$

where the z integral is a line integral with branch points. For azimuthal symmetry, the ray is also embedded in the radial-vertical plane and the ray's D/E angle, ϕ , is given by

$$\phi = \tan^{-1} (dr/dz)^{-1} = \tan \left[\frac{C_m^2}{C^2} - 1 \right]^{1/2} = \psi.$$

Hence for classical ray tracing, the D/E angle for both the ray and the wave normal are equal to each other. Therefore by azimuthal symmetry, the ray path is always normal to the wave fronts.

REFERENCES

1. E.R. Floyd, J. Acoust. Soc. Amer. 60, 801-809 (1976).
2. E.R. Floyd, J. Math. Phys. 20, 83-85 (1979).
3. E.R. Floyd, Phys. Rev. D, 25, 1547-1551 (1982).
4. E.R. Floyd, AIP document No. PAPS PRVDA-25-1547-20. (Supplement to Ref. 3: 15 pages which numerically describes the modified potential and effective action variable for the bound state.) Order by PAPS number and journal reference from American Institute of Physics, Physics Auxiliary Publication Service, 335 East 45th Street, New York, NY 10017. The price prepaid is \$1.50 for a microfiche or \$5.00 for photocopy. Airmail additional.

FIGURE CAPTIONS

1. The effective sound velocity profiles for a harmonic source at zero depth with $\omega = 50$ rad/s for initial D/E angles of 5° , 10° and 15° (i.e., $C_m = 1425.4242$ mps, 1441.9058 mps and 1470.0922 mps respectively). The sound velocity profile, C , is represented by the dashed curve.
2. The effective sound velocity profiles for a harmonic source at zero depth with an initial D/E angle of 10° (i.e., $C_m = 1441.9058$ mps) for $\omega = 5$ rad/s, 50 rad/s and 500 rad/s. The sound velocity profile, C , is represented by the dashed curve.
3. The rigorous ray trace for a harmonic sound source at zero depth, with $\omega = 50$ rad/sec, with an initial D/E angle of 10° for the sound velocity, C , exhibited on Figs. 1 and 2. The classical ray trace is represented by the dashed curve.
4. The deflection/elevation angle for the ray, ϕ , and wave normal, ψ , as a function of depth for the rigorous ray trace exhibited by Fig. 3. The deflection/elevation angle for classical ray trace is exhibited by the dashed curve.

Phase Velocity, m/s

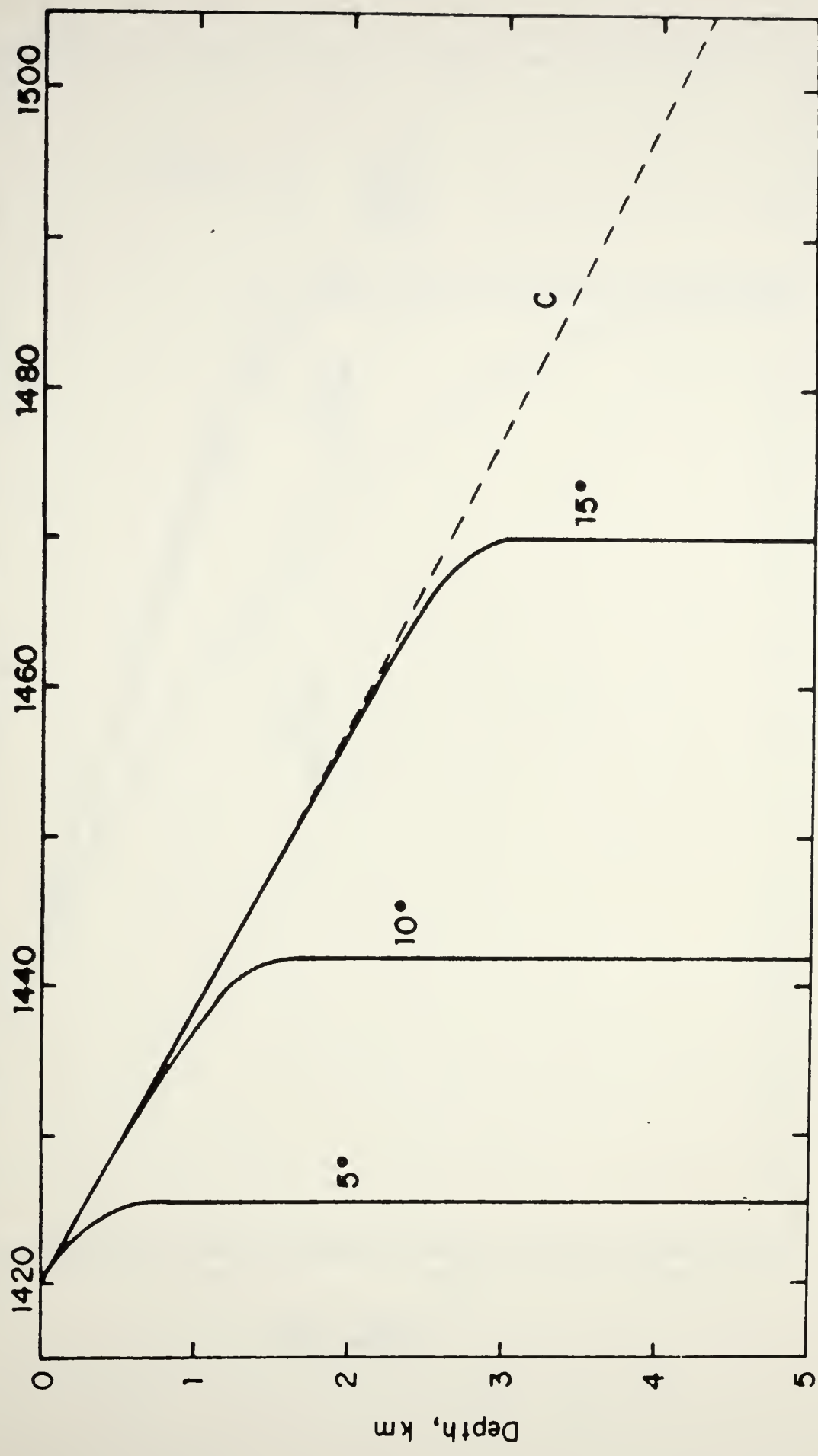
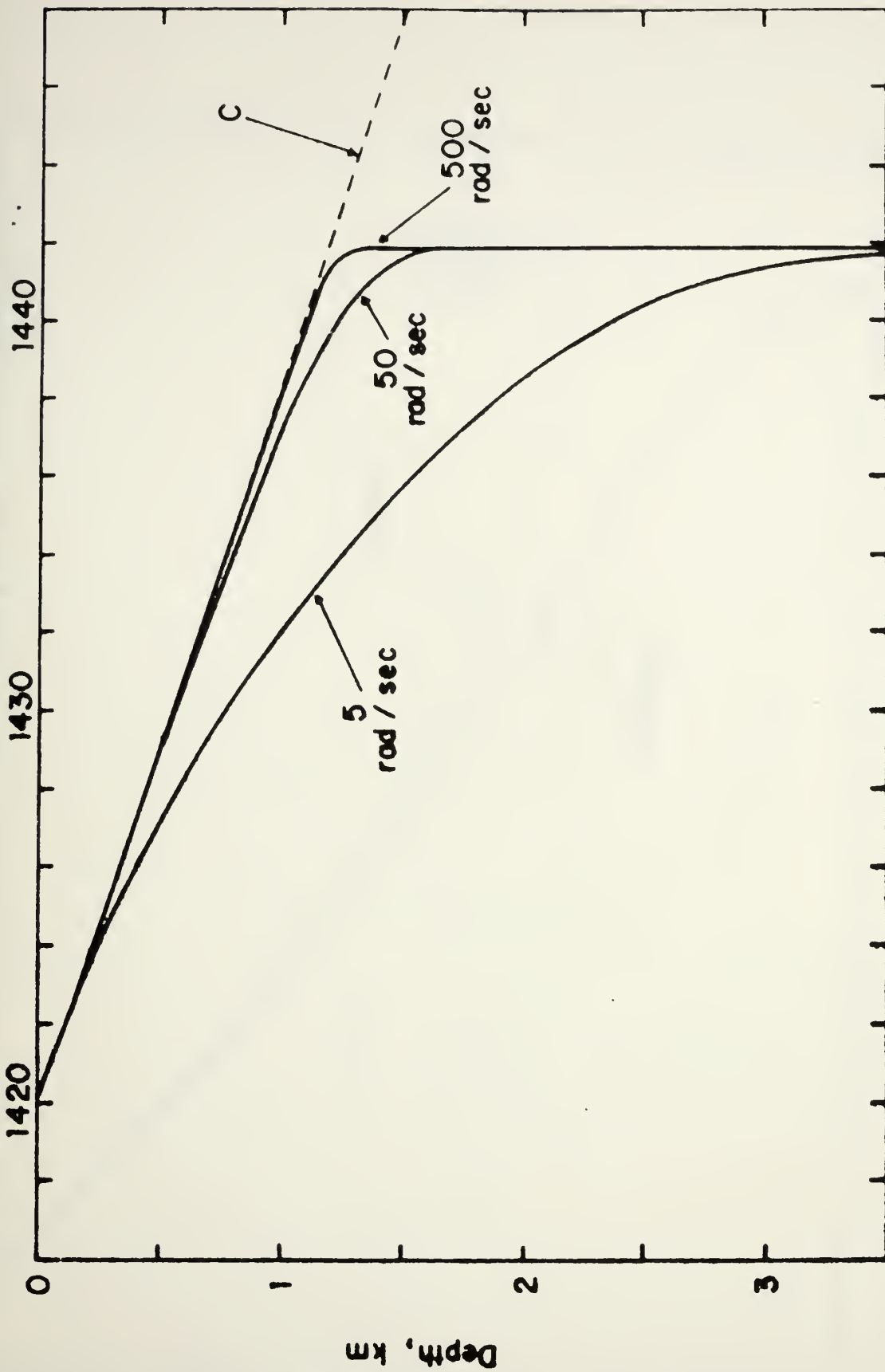


Fig. 1

Phase Velocity, mps



Depth, km

Fig. 2

HALF CYCLE RAY TRACE

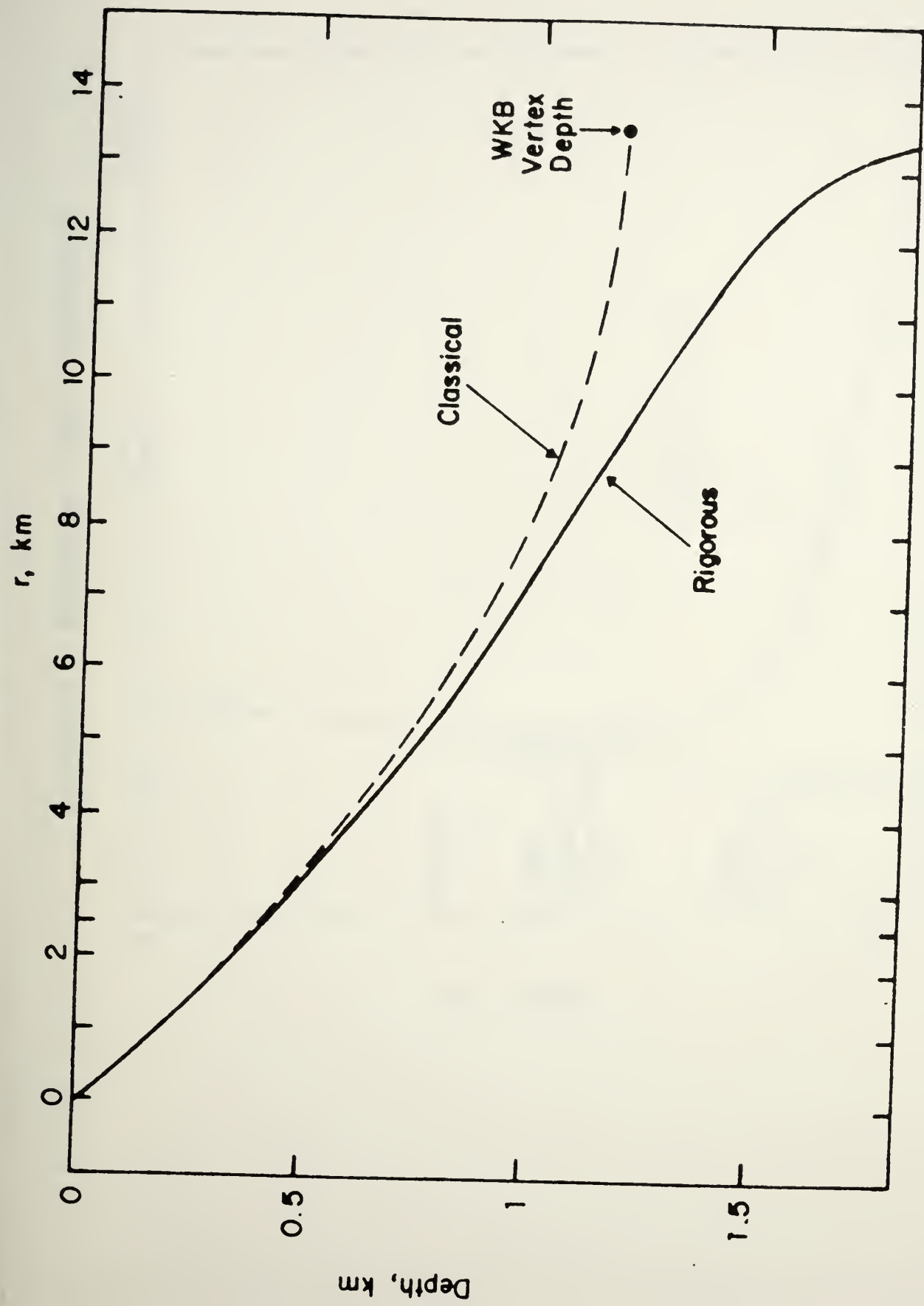


Fig. 3

Deflection / Elevation Angle, radians

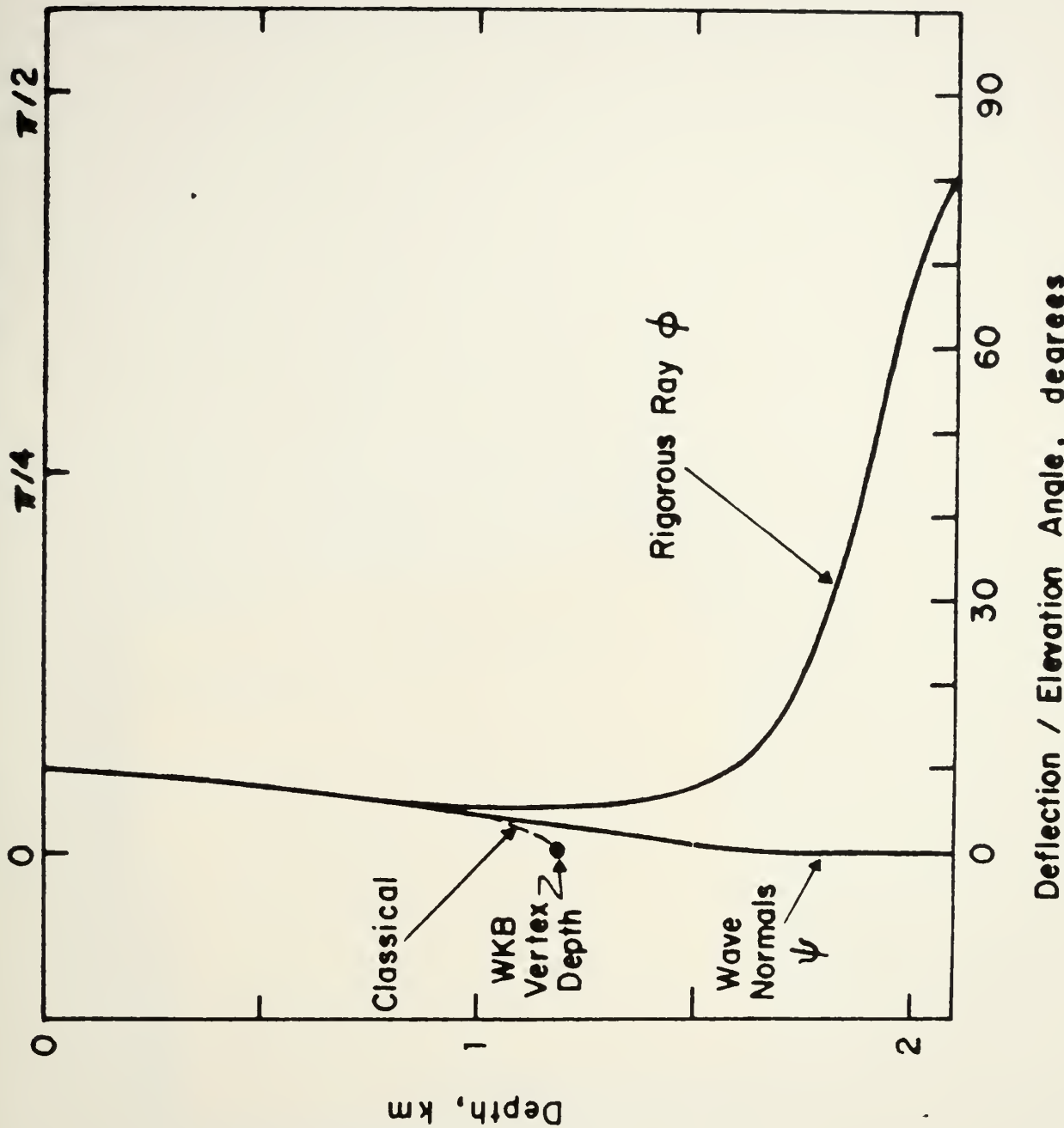


Fig. A



0237950
DUDLEY KNOX LIBRARY - RESEARCH REPORTS



5 6853 01058310 7